

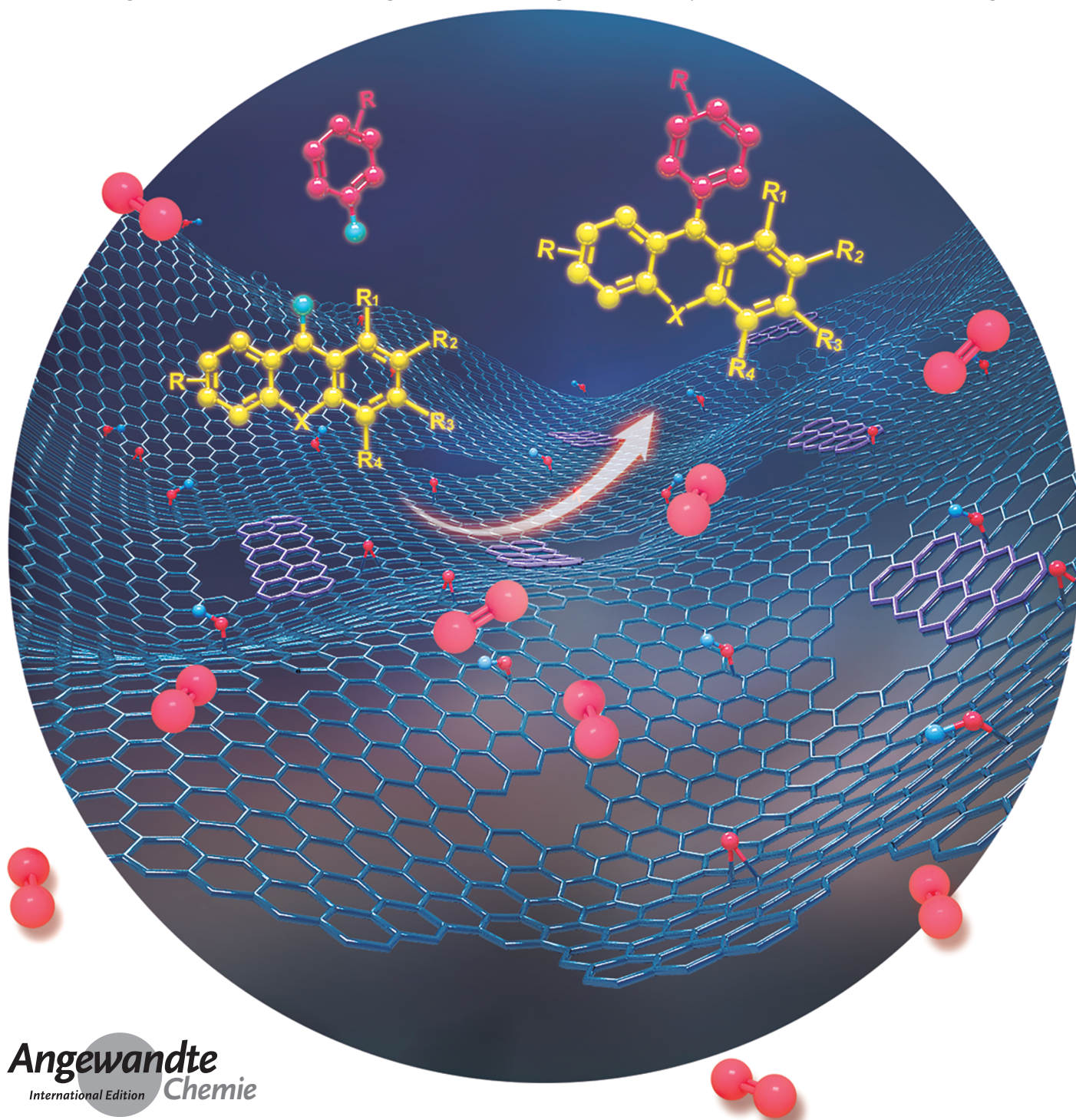
Carbocatalysis **Hot Paper**

International Edition: DOI: 10.1002/anie.201802548

German Edition: DOI: 10.1002/ange.201802548

Graphene-Oxide-Catalyzed Direct CH–CH-Type Cross-Coupling: The Intrinsic Catalytic Activities of Zigzag Edges

Hongru Wu⁺, Chenliang Su^{+,*}, Rika Tandiana, Cuibo Liu, Chuntian Qiu,
Yang Bao, Ji'en Wu, Yangsen Xu, Jiong Lu, Dianyuan Fan, and Kian Ping Loh^{*}

Angewandte
International Edition
Chemie

10848 Wiley Online Library

© 2018 Wiley-VCH Verlag GmbH & Co. KGaA, Weinheim

Angew. Chem. Int. Ed. 2018, 57, 10848–10853

Abstract: The development of graphene oxide (GO)-based materials for C–C cross-coupling represents a significant advance in carbocatalysis. Although GO has been used widely in various catalytic reactions, the scope of reactions reported is quite narrow, and the relationships between the type of functional groups present and the specific activity of the GO are not well understood. Herein, we explore CH–CH-type cross-coupling of xanthenes with arenes using GO as real carbocatalysts, and not as stoichiometric reactants. Mechanistic studies involving molecular analogues, as well as trapped intermediates, were carried out to probe the active sites, which were traced to quinone-type functionalities as well as the zigzag edges in GO materials. GO-catalyzed cross-dehydrogenative coupling is operationally simple, shows reusability over multiple cycles, can be conducted in air, and exhibits good functional group tolerance.

Carbocatalysis has become increasingly attractive in synthetic chemistry because of the prospect of replacing noble metal catalysts.^[1] The use of graphene oxide (GO) and its functionalized derivatives as carbocatalysts^[2–6] is of interest since the production of GO has entered the first phase of commercial production on the ton scale. The first landmark study on GO-based carbocatalysis by Bielawski et al. reported selective oxidation and hydration reactions.^[2] GO and its derivatives also exhibit excellent activity in the aerobic oxidation of amines^[3] and other oxidation reactions.^[4] Additionally, GO has been used as a bifunctional catalytic material when hybridized with a second metal catalyst. One major advantage of using GO compared to heterogeneous metal catalysts is that no additional support is needed since GO not only serves as a highly dispersible platform for anchoring metal nanoparticles but also provides synergetic catalytic sites.^[3b]

The activation of C–H bonds by carbocatalysts to form carbon–carbon and carbon–heteroatom bonds has recently emerged as a hot topic in carbocatalysis.^[1c] We and others have recently reported GO-catalyzed α -position C–H bond activation of primary amines with various nucleophiles,^[3b] alkylation of arenes with styrenes or alcohols,^[6a] and arylation of benzene with aryl iodides.^[6b] However, the development of

metal-free carbocatalysts for CH–CH-type cross-coupling has rarely been reported, although much desired.^[1c] Herein, we report that GO/rGO can be used as a heterogeneous, cost-efficient, and metal-free catalysts for the direct functionalization of the benzylic C–H bond of substituted xanthenes and thioxanthene with arenes in good yields and selectivity in open air. Mechanistic studies suggest that the defective domains with zigzag edges and quinone-type functionalities in GO materials are the most likely active sites for these reactions.

Our initial study was conducted using oxygen-rich GO-18 as the carbocatalyst for the aerobic cross-coupling of xanthene and 1,2-dimethoxybenzene.^[7] Performing the reaction at 100 °C for 24 h under solvent-free and open-air conditions afforded the coupling product in 46 % yield with xanthenone as the main byproduct. Replacing air with other oxidants, including *tert*-butyl hydroperoxide (TBHP), H₂O₂, and (2,2,6,6-tetramethylpiperidin-1-yl)oxyl (TEMPO), resulted in lower yields (Supporting Information, Table S1). To optimize the yield, a series of organic acid cocatalysts were screened to suppress the formation of the byproduct (Supporting Information, Table S1, Scheme S1). Other classes of carbocatalysts were also examined (Supporting Information, Table S1). The synergistic catalytic effect of GO-18 with TsOH·H₂O provided the best results (85 % NMR yield). The recovered GO-18 could be recycled and maintained its high catalytic activity (68 %) up to the fifth run (Supporting Information, Table S1). Performing the reaction in a glove box with ppm levels of O₂ reduced the yield to 26 %, which proves that O₂ is the terminal oxidant and that GO could only serve as an oxidant to a small degree. A control experiment conducted in the absence of catalyst produced 14 % yield, while using graphite (G) as the catalyst afforded only 6 % yield, indicating that the intrinsic properties of GO play an important role in the catalysis. Activated carbon (AC) also showed some catalytic activity (30 %), which probably stems from its surface oxygen functionalities and/or defects. However, base–acid-treated GO (ba-GO)^[3a] and reduced GO (rGO), which possess fewer oxygen functionalities than fully oxidized GO, also showed good catalytic activity (Figure 1; Supporting Information, Figure S1), suggesting that not all oxygen functional groups have vital roles in this catalytic system. Finally, the role of Mn impurities in GO materials has also been ruled out (Supporting Information, Figure S2).

To determine the relationship between the catalytic reactivity of GO and the density and types of oxygenated functionalities on the GO surface, the oxidation of GO samples was controlled systematically by using a reduced amount of oxidizing agent compared to the standard Hummer's procedure.^[8] For example, 1 g, 3 g, 6 g, and 10 g of KMnO₄ were used in place of the 18 g of KMnO₄ used in the normal Hummer's procedure, and the resulting products were named GO-1, GO-3, GO-6, GO-10, and GO-18 (or GO), respectively (Figure 2; Supporting Information, Figure S3). Figure 2a shows the X-ray photoelectron spectroscopy (XPS) C 1s spectra of GOs treated with different amounts of KMnO₄. The XPS C 1s spectra of GO-1, GO-3, and GO-6 indicate that mild oxidation produces mainly C–O species (that is, hydroxy and epoxide moieties), which

[*] Dr. H. Wu,^[†] Prof. Dr. C. Su,^[†] R. Tandiana, Dr. C. Liu, Dr. C. Qiu, Dr. Y. Xu, Prof. Dr. D. Fan
SZU-NUS Collaborative Center and International Collaborative Laboratory of 2D Materials for Optoelectronic Science & Technology Engineering Technology Research Center for 2D Material Information Function Devices and Systems of Guangdong Province College of Optoelectronic Engineering, Shenzhen University Shenzhen 518060 (China)
E-mail: chmsuc@szu.edu.cn

R. Tandiana, Dr. C. Liu, Dr. Y. Bao, Dr. J. Wu, Prof. Dr. J. Lu, Prof. Dr. K. P. Loh
Department of Chemistry, National University of Singapore 3 Science Drive 3, Singapore 117543 (Singapore)
E-mail: chmlhkp@nus.edu.sg

[†] These authors contributed equally to this work.

Supporting information and the ORCID identification number(s) for the author(s) of this article can be found under:
<https://doi.org/10.1002/anie.201802548>.

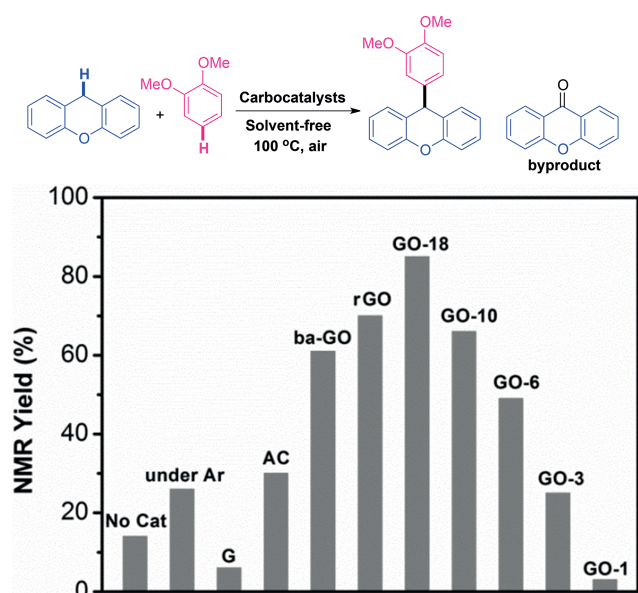


Figure 1. Carbocatalyzed cross-coupling of xanthene and arenes. The reaction was carried out with xanthene (0.5 mmol), 1,2-dimethoxybenzene (1 mmol), TsOH·H₂O (20 mol%), and catalyst (20 mg), with stirring at 100 °C for 24 h; NMR yield with ethylbenzene as the internal standard. Key: graphite (G), reduced GO (rGO), base–acid treated GO (ba-GO), activated carbon (AC).

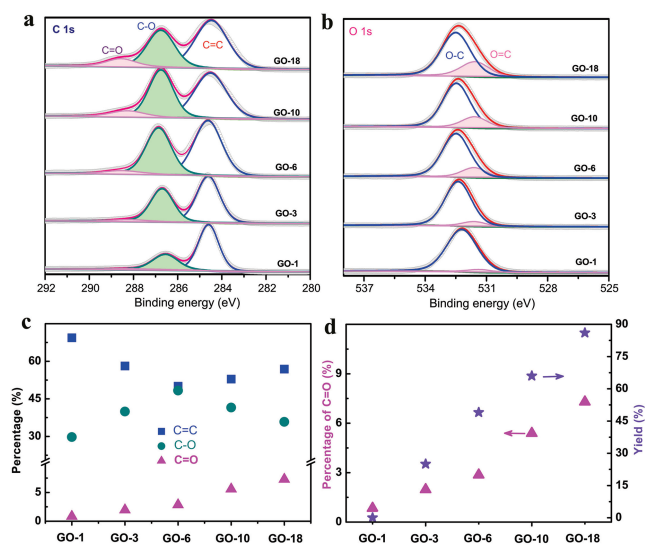
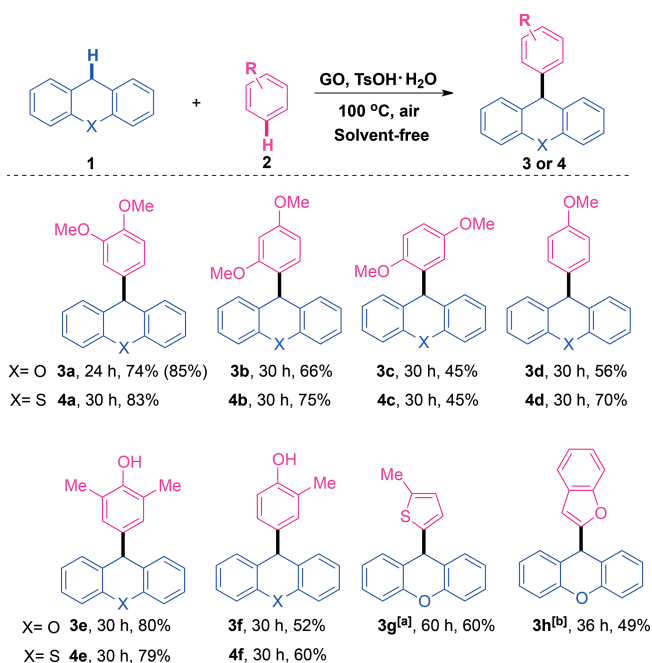


Figure 2. a) XPS C 1s spectra of GO materials. b) XPS O 1s spectra of GO materials. c) The concentration of oxygen functionalities was determined from the XPS C 1s spectra. d) The relationship between the density and type of C=O functionalities and the catalytic reactivity.

increase in density with the amount of oxidizing agent used. XPS spectra show that GO-1 has a significantly lower content of oxygenated functional groups compared to GO-3 and GO-6. Increasing the amount of oxidizing agent resulted in the formation of more C=O species (288.8 eV) than C–O species (286.6 eV), indicating the hydroxy and epoxide moieties were being converted to carbonyls and carboxylic groups. To determine the effect of the type of oxygen functionalities present on the activity of the catalyst,

GO-1 to GO-10 were used as catalysts under the same conditions as were used with GO-18 (Figure 1). The results show that the catalytic activity of GO is probably correlated to the density of C=O (Figures 1 and 2d) species. A more detailed mechanistic study is discussed in the proceeding text.

Using the optimized conditions, the effectiveness of GO as a catalyst for coupling various arenes with xanthene was assessed (Scheme 1). A series of electron-rich arenes, such as

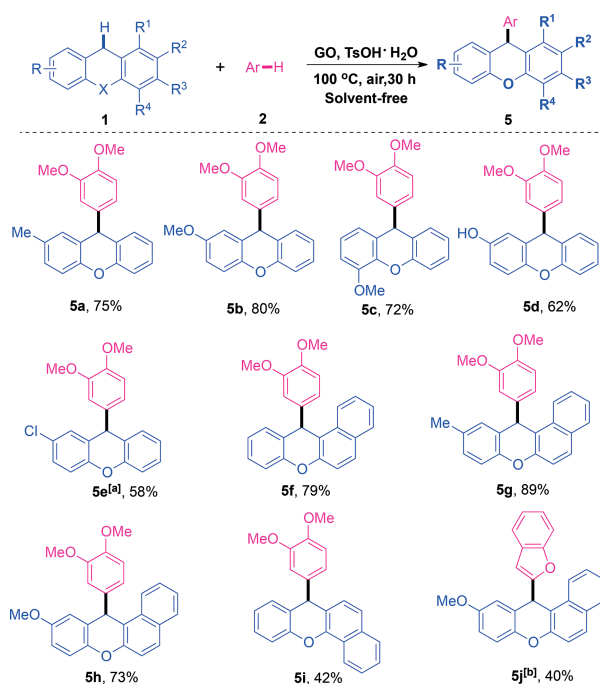


Scheme 1. The reaction was carried out with xanthene or thioxanthene (0.5 mmol), arene (1 mmol), TsOH·H₂O (20 mol%), and catalyst (20 mg), at 100 °C under solvent-free conditions. [a] Reaction at 60 °C. [b] Reaction at 75 °C.

meta- and *para*-dimethoxybenzene and anisole, was reacted with xanthene to afford the corresponding coupling products in 45–74% isolated yields. Acidic 2,6-xyleneol and *o*-cresol can be smoothly coupled with xanthene to produce the corresponding products in 80% and 52% yield, respectively. The synthetic utility of our method was further extended to the direct coupling of xanthene with heteroaromatic rings. High yields and excellent regioselectivity can be achieved in the direct CH–CH coupling of thioxanthene with a variety of electron-rich arenes, including heteroaromatic compounds (Scheme 1).

Subsequently, the scope of xanthenes with different substituents was examined. The catalyst shows good activity for a wide range of electron-donating groups, such as methoxy and methyl, and the desired coupling products were prepared in 72 to 80% yields. Hydroxy- and chloro-substituted xanthene produced coupling products in good yields. Benzofused xanthenes gave the corresponding products **5 f–5 g** in moderate to excellent yields (Scheme 2).

As discussed in the above section, the reactivity of GO is correlated to the concentration of quinone-type species (C=O) and has no obvious relationship with the content of



epoxide and hydroxy moieties. The use of molecular analogues allows us to mimic their catalytic domains, and the results are summarized in Table 1. Molecular analogues such as benzyl alcohol and 2,3-diphenyloxirane, which mimic the hydroxy and epoxide groups, showed low catalytic activity (Table 1, entries 1–2). Molecules with carboxylic acid groups, both with or without large conjugated domains, also showed little activity (Table 1, entries 3–4). Notably, polyaromatic hydrocarbons such as pyrene, coronene, and picene, which are characterized by aromatic structures and arm-chair edges, gave < 12% yield (Table 1, entries 5–7), whereas their zigzag-edged counterparts, such as tetracene and pentacene, exhibit higher reactivity. Anthraquinone, which incorporates both the zigzag edges and the C=O species, afforded the best performance among all the tested small-molecule analogues. This result echoes the previous observation that the reactivities of GO-related materials are linked to C=O species (Table 1, entries 10–11). These findings provide strong evidence that both the quinone-type functionalities and the zigzag edges in GO materials promote this coupling reaction.

Quinones are often suggested as the active sites/model catalysts for oxidations and dehydrogenations,^[9] whereas the catalytic behavior of the zigzag edges is much less studied.^[11] To investigate the exclusive role of zigzag edges in GO, the oxygen functionalities were removed by high-temperature annealing (> 800 °C). Fourier transform infrared (FTIR) analysis (Figure 3a) shows greatly reduced contents of epoxide and hydroxy species after this treatment, and confirms the successful removal of the C=O functionalities (ca. 1650–1800 cm⁻¹); this conclusion is also supported by XPS analysis in Figure 3b where the ratio of C:O is now increased to 30:1. Because of the thermally processed

desorption of oxygen species as CO or CO₂, vacancies are created. The aggregation of these vacancies creates nanopores, which are believed to be terminated by zigzag edges. To confirm this, we analyzed the atomic structures of the pores using scanning tunneling microscopy (STM). Figure 3c reveals the honeycomb lattice of the thermally treated GO basal plane. Most importantly, the edges of the pores contain straight edges that are aligned with the zigzag axis in graphene, thus these are zigzag edges (marked by white dashed lines). An atom-resolved STM image and the structural model of the zigzag edge are provided in Figure 3c. The fact that these zigzag edges play important roles in the catalysis was confirmed by testing the catalytic reactivity of the rGO in the cross-coupling reactions of xanthene and arenes, in which the coupled products were obtained in 83% and 80% yields using rGO annealed at 800 °C and 1000 °C, respectively. High-temperature annealing at 1000 °C removes most of the oxygen functionalities, but the catalytic activity is only marginally reduced relative to untreated GO, which provides further proof that the zigzag edges play a major role in the catalysis.

Table 1: Evaluation of small molecular analogue mimics.^[a]

Entry	Small molecule	Mimicking sites	Yield [%] ^[b]
1		Alcohol	20
2		Epoxide	22
3		Carboxylic acid	20
4		Carboxylic acid	14
5		Conjugation domain	12
6		Conjugation domain	10
7		Arm-chair edge	3
8		Zigzag edge	50
9		Zigzag edge	54
10		Quinones	76
11		Quinones	60

[a] The reaction was carried out with xanthene (0.5 mmol), arene (1 mmol), TsOH·H₂O (20 mol%), and catalyst (20 mg) at 100 °C.
[b] NMR yield with anisole as the internal standard.

A possible mechanism is presented in Figure S4 (Supporting Information), involving the following key steps: 1) the

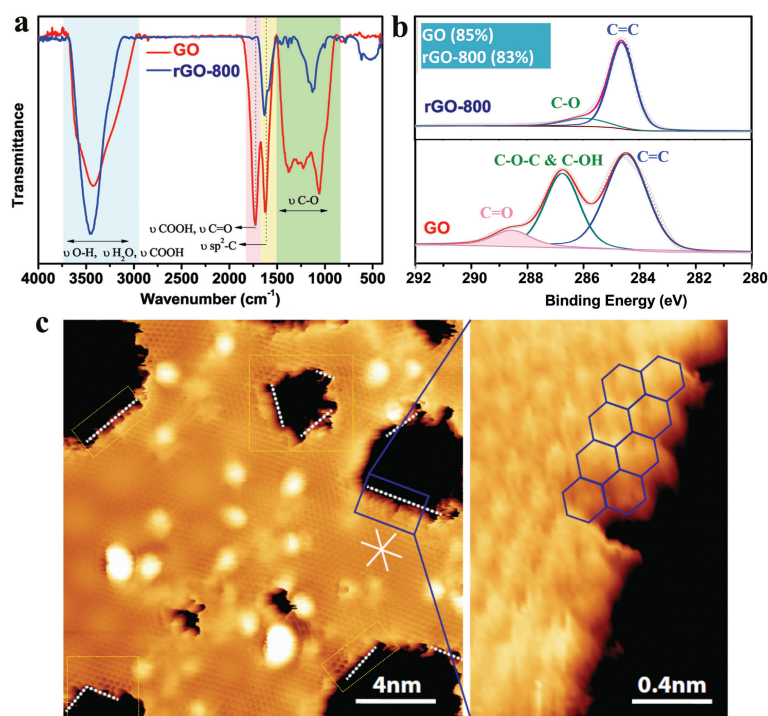


Figure 3. a) Transmission infrared spectra of GO (red) and rGO-800 (blue). b) A typical STM image of GO on highly oriented pyrolytic graphite (HOPG) and annealed at high temperature. c) Atom-resolved STM image of the zigzag edge (marked); the structural model of the graphene lattice is superimposed.

activation of xanthene by rGO-O₂ or tetracene-O₂ intermediate, and 2) the formation of a transition state in which the arene nucleophile is prepositioned for C–C bond formation by π – π stacking interactions with graphene, which is consistent with prior literature.^[6a] rGO with zigzag edges is expected to promote the oxidation of xanthene to a peroxide intermediate by the following steps. Firstly, the absorption of O₂ onto the defective edges of rGO is believed to form the intermediate rGO-O₂. The conjugated electrons of xanthene favor its absorption onto graphene and formation of a complex with rGO-O₂ to produce the xanthene peroxide intermediate. The synergistic effect of acids and rGO helps to promote the coupling of xanthene peroxide intermediate with arenes. The use of tetracene as a molecular analogue for the zigzag edges of graphene allows us to probe the reaction mechanism by isolation of the intermediates. In this case, the reduced product 5,12-dihydro-tetracene confirmed the ability of the zigzag edges to extract hydrogen (deuterium) in competition with O₂, in which the extraction may occur via the same intermediate tetracene-O₂ species. The interaction between xanthene and rGO-O₂ is further supported by the small-molecule-mimicking experiments and the detection of superoxide radical (Supporting Information, Figure S5 and S6). One major difference in the catalytic activity of the tetracene analogue compared to that of graphene is that, once the former is reduced, it loses its catalytic activity, whereas the much longer conjugated aromatic network in graphene allows the catalyst to be recycled multiple times (Supporting Information, Figure S7).

Theoretical calculations suggest that, because of the localized π states in zigzag edges and its closeness to the Fermi level, the zigzag edges are radical-like;^[10a] thus, these are potentially active catalyst sites. Using a combination of bias-dependent STM studies and density functional theory (DFT) calculations, Enoki et al. suggested that oxygenated zigzag edges change the spatially localized edge state in the zigzag edges into an extended one on account of the additional π conjugation from C=O functionalities.^[10b] The improved “metallicity” of these oxidized edge sites^[10c] should further improve the catalytic properties of the edge sites. Therefore, the coexistence of ketonic functionalities and zigzag edges can have synergetic effects in catalysis, although our studies show that substantial removal of the C=O functionalities does not degrade the catalytic activity of the zigzag edges significantly since the latter can participate directly in dehydrogenation reactions because of its radical-like nature. As opposed to oxygenated functionalities in GO, which sometime act as stoichiometric reactants and become consumed in the reactions, the zigzag sites are relatively robust. Defective edges could be generated by heating because of the decomposition of oxygenated functionalities and generation of pores, thus zigzag-edged catalysts can be reused in multiple catalytic cycles. Previous catal-

ysis studies on GO materials have largely focused on the role of oxygenated groups; this work suggests that more attention should be focused on the role of zigzag edge sites instead, since these qualify as true catalytic sites in carbocatalysts.

In summary, we have developed a carbocatalyzed CH–CH-type cross-coupling reaction of xanthenes (or thioxanthenes) and arenes that is operationally simple and has good functional group tolerance. Mechanistic studies revealed that the catalytic reactivity is promoted by C=O species as well as the zigzag edges in GO. STM studies reveal that thermally processed GO possess a high density of zigzag edges around defective sites and, despite its lack of C=O functionalities, its catalytic activity (83%) was only slightly lower than that of GO (85%), which indicated that the intrinsic catalytic activities of the zigzag edges are quite high. Our study suggests that, under acidic conditions, porous carbon materials with a high density of zigzag edge sites can serve as true carbocatalytic models for C–C couplings.

Acknowledgements

C.S. is grateful for financial support from the NNSFC (51502174), Shenzhen Peacock Plan (Grant No. KQJSCX20170727100802505, KQTD2016053112042971). K.P.L. thanks NRF Investigator Award (Award No. NRF-NRF12015-01) from National Research Foundation, Singapore, for support. K.P.L. also thanks Shenzhen peacock plan KQTD2016053112042971. D.F. thanks the Educational Com-

mission of Guangdong Province (2016KCXTD006 and 2016KSTCX126).

Conflict of interest

The authors declare no conflict of interest.

Keywords: C–C coupling · graphene oxide · metal-free catalysis · zigzag edges

How to cite: *Angew. Chem. Int. Ed.* **2018**, *57*, 10848–10853
Angew. Chem. **2018**, *130*, 11014–11019

- [1] a) D. S. Su, S. Perathoner, G. Centi, *Chem. Rev.* **2013**, *113*, 5782–5816; b) D. H. Deng, K. S. Novoselov, Q. Fu, N. F. Zheng, Z. Q. Tian, X. H. Bao, *Nat. Nanotechnol.* **2016**, *11*, 218–230; c) S. Navalon, A. D. Hakshinamoorthy, M. Alvaro, H. Garcia, *Chem. Rev.* **2014**, *114*, 6179–6212; d) C. L. Su, K. P. Loh, *Acc. Chem. Res.* **2013**, *46*, 2275–2285; e) D. R. Dreyer, C. W. Bielawski, *Chem. Sci.* **2011**, *2*, 1233–1240; f) D. S. Su, G. D. Wen, S. C. Wu, F. Peng, R. Schlogl, *Angew. Chem. Int. Ed.* **2017**, *56*, 936–964; *Angew. Chem.* **2017**, *129*, 956–985; g) S. Navalon, A. Dhakshinamoorthy, M. Alvaro, M. Antonietti, H. Garcia, *Chem. Soc. Rev.* **2017**, *46*, 4501–4452; h) P. Tang, G. Hu, M. Z. Li, D. Ma, *ACS Catal.* **2016**, *6*, 6948–6958.
- [2] D. R. Dreyer, H. P. Jia, C. W. Bielawski, *Angew. Chem. Int. Ed.* **2010**, *49*, 6813–6816; *Angew. Chem.* **2010**, *122*, 6965–6968.
- [3] a) C. L. Su, M. Acik, K. Takai, J. Lu, S. J. Hao, Y. Zheng, P. P. Wu, Q. L. Bao, T. Enoki, Y. J. Chabal, K. P. Loh, *Nat. Commun.* **2012**, *3*, 1298–1307; b) C. L. Su, R. Tandiana, J. Balapanuru, W. Tang, K. Pareek, C. T. Nai, T. Hayashi, K. P. Loh, *J. Am. Chem. Soc.* **2015**, *137*, 685–690.
- [4] a) Y. J. Gao, G. Hu, J. Zhong, Z. J. Shi, Y. S. Zhu, D. S. Su, J. G. Wang, X. H. Bao, D. Ma, *Angew. Chem. Int. Ed.* **2013**, *52*, 2109–2113; *Angew. Chem.* **2013**, *125*, 2163–2167; b) X. H. Li, J. S. Chen, X. C. Wang, J. H. Sun, M. Antonietti, *J. Am. Chem. Soc.* **2011**, *133*, 8074–8077.
- [5] A. Primo, F. Neatu, M. Florea, V. Parvulescu, H. Garcia, *Nat. Commun.* **2014**, *5*, 5291–5300.
- [6] a) F. Hu, M. Patél, F. X. Luo, C. Flach, *J. Am. Chem. Soc.* **2015**, *137*, 14473–14480; b) Y. J. Gao, P. Tang, H. Zhou, W. Zhang, H. J. Yang, N. Yan, G. Hu, D. H. Mei, J. G. Wang, D. Ma, *Angew. Chem. Int. Ed.* **2016**, *55*, 3124–3128; *Angew. Chem.* **2016**, *128*, 3176–3180.
- [7] a) A. Printér, M. Klussmann, *Adv. Synth. Catal.* **2012**, *354*, 701–711; b) B. Schweitzer-Chaput, A. Sud, S. Dehn, P. Schulze, M. Klussmann, *Angew. Chem. Int. Ed.* **2013**, *52*, 13228–13232; *Angew. Chem.* **2013**, *125*, 13470–13474.
- [8] a) S. Pattison, E. Nowicka, U. N. Gupta, G. Shaw, R. J. Jenkins, D. J. Morgan, D. W. Knight, G. J. Hutchings, *Nat. Commun.* **2016**, *7*, 12855–12864; b) H. L. Poh, F. Sanek, A. Ambrosi, G. Zhao, Z. Sofer, M. Pumera, *Nanoscale* **2012**, *4*, 3515–3522.
- [9] a) A. E. Wendlandt, S. S. Stahl, *Angew. Chem. Int. Ed.* **2015**, *54*, 14638–14658; *Angew. Chem.* **2015**, *127*, 14848–14868; b) A. E. Wendlandt, S. S. Stahl, *J. Am. Chem. Soc.* **2015**, *137*, 14473–14480.
- [10] a) D. E. Jiang, B. G. Sumpter, S. Dai, *J. Chem. Phys.* **2007**, *126*, 134701–134708; b) M. Ohtsuka, S. Fujii, M. Kiguchi, T. Enoki, *ACS Nano* **2013**, *7*, 6868–6874; c) O. Hod, V. Barone, J. E. Peralta, *Nano Lett.* **2007**, *7*, 2295–2299.

Manuscript received: February 28, 2018

Revised manuscript received: April 15, 2018

Accepted manuscript online: May 10, 2018

Version of record online: June 7, 2018